



HAL
open science

Modeling of pellet cladding interaction during power ramps in pressurized water reactors

O. Diard, S. Leclercq, Gilles Rousselier, Farida Azzouz, G. Cailletaud

► **To cite this version:**

O. Diard, S. Leclercq, Gilles Rousselier, Farida Azzouz, G. Cailletaud. Modeling of pellet cladding interaction during power ramps in pressurized water reactors. SMIRT 16, International Association for Structural Mechanics in Reactor Technology, Aug 2001, Washington DC, United States. hal-04062197

HAL Id: hal-04062197

<https://hal.science/hal-04062197>

Submitted on 7 Apr 2023

HAL is a multi-disciplinary open access archive for the deposit and dissemination of scientific research documents, whether they are published or not. The documents may come from teaching and research institutions in France or abroad, or from public or private research centers.

L'archive ouverte pluridisciplinaire **HAL**, est destinée au dépôt et à la diffusion de documents scientifiques de niveau recherche, publiés ou non, émanant des établissements d'enseignement et de recherche français ou étrangers, des laboratoires publics ou privés.

Modeling of pellet-cladding interaction during power ramps in pressurized water reactors

O. DIARD^a, *S. LECLERCQ*^b, *G. ROUSSELIER*^b, *F. AZZOUZ*^a, *G. CAILLETAUD*^a

^a Centre des Matériaux Pierre-Marie Fourt, Ecole Nationale Supérieure des Mines de Paris, UMR CNRS 7633, BP 87, F-91003 Evry Cedex, France

^b Electricité de France, Division Recherche et Développement, Les Renardières, Route de Sens, BP 1, F-77818 Moret sur Loing Cedex, France

ABSTRACT

Pellet-cladding interactions (PCI) which can occur during power transients (Class 2 incidental operating conditions) in nuclear reactors may lead to Zircaloy-4 cladding failure by stress corrosion cracking. Indeed under transient power conditions, a rapid increase of the linear heat generation rate (i.e. thermal power released per unit length) induces dilatations of fuel pellets and a strong mechanical pellet-cladding interaction. Observations of cracks on inner surfaces of failed claddings show a preferential localisation in continuity of radial fuel cracks, with a higher number of occurrences at the vicinity of pellet-pellet interfaces.

Acceptable maximum power levels and rate of power increases are often defined according to the notion of threshold hoop stress. The aim of this work is thus to propose a numerical simulation of representative power ramps to provide a good estimation of local strain and stresses induced by fuel pellet extension. This paper presents several simulations of power ramps by the Finite Element method. Attention was paid to the description of irradiation creep and creep under high stress of the Zy-4 cladding with two specific anisotropic viscoplastic models including irradiation damage effects. Moreover the viscoplastic behavior of the pellet was considered.

In the first part, 2D calculations focus on the description of the stress concentration that occurs in the inner surface due to the presence of fuel pellet cracks. Results show that the local hoop stress is four to six times higher than the mean hoop stress. Effects of frictions conditions are especially analyzed. It appears that a high friction coefficient (due to the formation of solid compounds such U-Cs-Zr) drastically increases stress and strain levels in the cladding inner surface. In the second part, a 3D modeling is also proposed to complete 2D investigations and to study geometrical aspects of PCI, such as the evolution of pellet cladding gap and fuel rod radial deformation during the ramp, especially the main and secondary ridges of the cladding. Calculations taking into account a realistic deformation of the pellet provide a better agreement with experimental data with respect to classical axysymmetric 2D calculations. These simulations provide a good description of the gap closure kinetics and allow to evaluate respective effects of pellet creep and gas swelling in the appearance of the secondary ridge of the cladding.

INTRODUCTION

Fuel rods of pressurized water reactor (PWR) are composed of Uranium dioxide pellets set in Zircaloy-4 cladding. Under transient power conditions, a rapid increase of the temperature induces dilatations of fuel pellets and a mechanical pellet-cladding interaction. In addition, fuel breaks under the thermal gradient which appears in the pellet from the first cycle. Hence, fragments indent the inner surface of the cladding and induce local stress concentrations. This phenomenon of PCI occurs in a corrosive environment, composed of accumulated volatile fission products such as iodine, and may lead to stress corrosion cracking.

The risk of cladding failure is still a limitation for the management of the nuclear network. Acceptable maximum power levels and rate of power increases have been defined according to the notion of threshold hoop stress. In view of increasing fuel assemblies performances (burn-up from 40 GWd/t up to 60 GWd/t) and to insure the integrity of the cladding, which constitutes the first protection against nuclear wastes, large research programs have been set up. Intensive studies have been made to understand damage phenomena associated to the cladding failure [1, 2, 3], experimental determinations of the threshold stress and studies of the effects of microstructural properties of Zircaloy have also been published [4, 5] and attempts for failure prediction models have been proposed [6, 7].

The aim of this work is to propose a numerical simulation of representative power ramps with an anisotropic viscoplastic model for the Zircaloy-4 cladding, to provide a good estimation of strain and stresses induced by fuel pellet extension. The first 2D calculations focus on the description of the stress concentration that occurs in

the inner surface due to the presence of fuel pellet cracks. Effects of frictions conditions are especially analysed. The inner surface state and the formation of solid compounds between Zr and UO_2 can modify the friction coefficient in a wide range, which largely modifies the hoop stress in the critical region. Efficient 2D and 3D contact algorithms are used to take this phenomenon into account. A 3D modeling is also proposed to complete 2D investigations and to study geometrical aspects of PCI, such as the evolution of the pellet cladding gap and the fuel rod radial deformation during the ramp.

MATERIAL BEHAVIOR

Uranium dioxide fuel pellet

Above about 1300°C Uranium dioxide becomes viscoplastic. To describe fuel mechanical behavior during power ramps, wich includes, creep, but also hardening and relaxation, the viscoplastic model used for UO_2 has been improved with respect to more classical creep laws [8]. The following is a simplified version of that model. The isotropic elasto-viscoplastic model is presented by Eqs (1-3):

$$\dot{\bar{\epsilon}}^t = \dot{\bar{\epsilon}}^e + \dot{\bar{\epsilon}} \quad \dot{\bar{\epsilon}}^e = \frac{1+\nu}{E} \dot{\bar{\sigma}} - \frac{\nu}{E} \text{trace}(\dot{\bar{\sigma}}) \quad (1)$$

$$\bar{\sigma} = \left\{ \frac{3}{2} \bar{\sigma}' : \bar{\sigma}' \right\}^{\frac{1}{2}} \quad (2)$$

$$\dot{\bar{\epsilon}} = (1 + L \cdot \Phi) \cdot \left(\frac{\bar{\sigma}}{K_0 \bar{\epsilon}^{1/m}} \right)^n \exp(-Q/RT) \quad (3)$$

Eq. 1 describes the partition of the total strain rate into elastic and plastic rate and the Hooke's law. The viscoplastic flow is described by a power law of the von Mises stress, defined from the deviatoric stress $\bar{\sigma}'$ (Eq. 2) and includes a strain hardening term (Eq. 3). In addition, a linear modification is introduced with the neutron flux Φ in order to describe the acceleration of the creep deformation under irradiation due to the neutron flux. A multiplicative Arrhenius term is added to take the temperature sensitivity into account. Coefficients of this model have been identified out of pile on unirradiated UO_2 using some compression tests.

Zircaloy-4 cladding

Metallurgical properties

Zircaloy-4 is a zirconium based alloy (hexagonal lattice under 800°C), with tin, iron, chrome and oxygen as main alloy elements. Zy-4 used as reference for this study is the alloy used for the fabrication of the Framatome second generation cladding AFA-2G.

Zircaloy cladding presents high morphological and textural anisotropies due to its machining by rolling. For this reason tubes undergo a thermal treatment of about 2 h at 460°C to reduce this anisotropy. The crystallographic texture of tubes in the cold worked stress relieved state (CWSR) presents nevertheless preferential orientations of the $\{0002\}$ axis at $\pm 40^\circ$ in the (r,θ) plane and at $\pm 15^\circ$ in the (r,z) plane and a morphological anisotropy with grains of $5 \mu\text{m}$ long for about $2 \mu\text{m}$ large. This anisotropy induces a significant anisotropy of the mechanical properties.

In addition, physical mechanisms responsible for the deformation of Zy-4 cladding highly depend on the level of stress. Under irradiation the microstructure of Zircaloy is changing due to the neutron flux. Gilbon and Simono [9] have reviewed the main effects of this damage and this will not be discussed in this paper. Nevertheless we can distinguish the irradiation growth, which refers to the dimensional changes at constant volume of an unstressed material under irradiation [10], the irradiation creep under external stress during base operating conditions (stress under 100 MPa) induced by specific interactions between dislocations climb and glide and irradiation defects, and the thermal creep for stress above 200 MPa (typically during power ramps).

Description of the anisotropic viscoplastic model for thermal creep

A specific anisotropic viscoplastic model has been developed, first for an austenitic stainless steel and for Zircaloy tubes after the penultimate laminate pass, and finally identified for the material of this study, between 350 and 400°C . This model is a unified viscoplastic model with only one inelastic strain. The introduction

of internal variables allows the description of monotonic and cyclic hardening and also of recovery of internal stresses. The mathematical formulation of the several constitutive equations is summarized in Eqs (4-10):

The strain rate respects the normality rule with a flow direction derived from the effective stress $\underline{g}' - \underline{X}'$, where the superscript ' denotes the deviatoric part of the tensor. This direction is modified by the fourth order tensor $\underline{\underline{M}}$ introduced in the definition of the equivalent stress $\overline{\sigma - X}$ to take account of anisotropy (Eqs 4-6).

The evolution of the internal stress \underline{X} is described with three variables of kinematic hardening, including recovery terms. Those equations are modified with three tensors $\underline{\underline{N}}$, $\underline{\underline{Q}}$, $\underline{\underline{R}}$ (respectively for the hardening, dynamic recovery and static recovery variables), to describe the center of the elastic domain and the induced anisotropy (Eqs 7-9).

- Viscoplastic flow:

$$\underline{\dot{\varepsilon}} = \frac{3}{2} \bar{\varepsilon} \frac{\underline{\underline{M}} : (\underline{g}' - \underline{X}')}{\overline{\sigma - X}} \quad (4)$$

$$\bar{\varepsilon} = \dot{\varepsilon}_0 \left\{ \sinh \left(\frac{\overline{\sigma - X}}{N_0} \right) \right\}^n \quad (5)$$

with $\overline{\sigma - X} = \left\{ \frac{3}{2} (\underline{g}' - \underline{X}') : \underline{\underline{M}} : (\underline{g}' - \underline{X}') \right\}^{\frac{1}{2}}$ (6)

- Kinematic hardening and recovery variables evolutions:

$$X = p \alpha \quad X^{(1)} = p_1 \alpha^{(1)} \quad X^{(2)} = p_2 \alpha^{(2)} \quad (7)$$

$$\begin{aligned} \dot{\alpha}'^{(2)} &= \frac{2}{3} Y^* \underline{\underline{N}} \underline{\dot{\varepsilon}} - \underline{\underline{Q}} \underline{X}'^{(2)} \\ \dot{\alpha}'^{(1)} &= \frac{2}{3} Y^* \underline{\underline{N}} \underline{\dot{\varepsilon}} - \underline{\underline{Q}} (\underline{X}'^{(1)} - \underline{X}'^{(2)}) \end{aligned} \quad (8)$$

$$\begin{aligned} \dot{\alpha}' &= \frac{2}{3} Y^* \underline{\underline{N}} \underline{\dot{\varepsilon}} - \underline{\underline{Q}} (\underline{X}' - \underline{X}'^{(1)}) - \lambda_r \sinh \left(\left(\frac{\bar{\alpha}}{\alpha_0} \right)^{m_0} \right) \underline{\underline{N}} \underline{\underline{R}} \frac{\alpha'}{\bar{\alpha}} \\ \text{with } \bar{\alpha}' &= \left\{ \frac{3}{2} \alpha' : \underline{\underline{R}} : \alpha' \right\}^{\frac{1}{2}} \end{aligned} \quad (9)$$

- Isotropic hardening description, where Y^* is the yield stress:

$$Y^* = Y_0 + Y_{iso} \quad \text{with} \quad \dot{Y}_{iso} = b (Y_{iso}^{sat} - Y_{iso}) \bar{\varepsilon} \quad (10)$$

The parameters of this model have been identified by I. Schäffler [11] between 350 °C and 400 °C, which corresponds to the cladding base operating temperature.

Irradiation creep model

Irradiation creep involves irradiation defects as vacancies and interstitials. Matthews and Finnis [12] have described this phenomenon using dislocation climb controlled by the stress-modified absorption of defects (stress induced preferential absorption). Electricité de France (EDF) developed a modified viscoplastic model to take the neutron flux into account. An anisotropic version is presented with Eqs (11-12):

$$\underline{\dot{\varepsilon}} = \frac{3}{2} \bar{\varepsilon} \frac{\underline{\underline{A}} : (\underline{g}')}{\bar{\sigma}} \quad \text{with} \quad \bar{\sigma} = \left\{ \frac{3}{2} \underline{g}' : \underline{\underline{A}} : \underline{g}' \right\}^{\frac{1}{2}} \quad (11)$$

$$\bar{\varepsilon} = \left(\frac{\bar{\sigma}}{(K \cdot \Phi + L) \bar{\varepsilon}^{1/m}} \right)^n \exp(-Q/RT) \quad (12)$$

This is a viscoplastic model quite similar to the model used for UO₂, with a multiplicative term for strain hardening and the appearance of the neutron flux Φ in the flow rate to introduce a decrease of the flow rate with respect to irradiation evidenced in experimental reactors. The flow direction is modified by the tensor $\underline{\underline{A}}$ in order

to describe plastic anisotropy. Identification has been made by EDF.

Explicite and implicite implementations of these models have been made in the F.E. code ZeBuLon used for calculations presented in this paper.

MODELLING OF REPRESENTATIVE POWER RAMPS

Power history

The sensitivity of the fuel rod to cladding failure depends on the burn-up and more exactly on the complete power history. The risk of failure seems to increase up to 35 GWd/tU and decrease for higher burn-up and to be maximum for intermediate burn-up (20 to 35 GWd/tU), which corresponds to about two or three operating cycles. Moreover it is well known that the initial gap between the pellet and the cladding is closed after one or two cycles, inducing pellet cladding mechanical interaction. For this reason, analytical ramping tests are performed on refabricated rods having been irradiated in base operating conditions (typically 15 to 25 kW m⁻¹). This ramp test is defined by the maximum power (P_{max}) to be reached, the increment of power (ΔP) and the rate of increase (\dot{P}). Typical values are about 40 kWm⁻¹ for P_{max} , 20 kWm⁻¹ for ΔP and about 0.2 kWm⁻¹s⁻¹ for \dot{P} .

In order to establish the loading and boundary conditions of the 2D and 3D calculations, a first step has to be made, which provides an estimation of the temperature gradients in the fuel and in the cladding during the ramp. The 1.5D E.F. code developed by EDF, CYRANO3, has been used for it. This code describes several phenomena, such as nuclear power distribution and thermal diffusion in the fuel rod. Calculated thermal profiles for several linear heat generation rate (LHGR) are reported in Fig. 2.

Friction conditions and geometrical description

The modelling of pellet cladding interaction includes also a description of the fuel fragmentation during the first and the second cycles and the friction conditions between Uranium dioxide and Zirconium. The friction conditions are of first importance. The opening of radial fuel crack due to heterogeneous thermal expansion induces a shear component in the inner surface of the cladding, when the gap is closed. The magnitude of the shear stress and of the induced hoop stress in front of the crack depends largely on the friction coefficients. It is impossible to measure this coefficient under operating conditions, but one can estimate it to 0.7 for metal-oxyde interaction. In addition, a range of 0.5 to 1.5 is defined in order to take into account the formation of solid compounds such as U-Cs-Zr between the pellet and the cladding as well as the external degradation of the fuel pellet (rim effect) which reduces the friction coefficient.

In the same way, the number of fragments is a significant parameter for determining hoop stress in the cladding. Indeed, the fragments distribution modifies their kinematic motion before the ramp, when the gap is closed, which can induce an offset of the cladding radial displacement. The number of eight fragments is chosen for the calculation. This number corresponds to an intermediate configuration for 20 kWm⁻¹ and 40 kWm⁻¹, according to a parametric study of Oguma [13].

Observations of cracks on inner surfaces of failed claddings show a preferential localisation in continuity of radial fuel cracks, with a higher number of observations at the vicinity of pellet-pellet interfaces. Indeed indentation of pellet fragments on both sides of the fuel crack induces a stress concentration and the fuel crack appears as a preferential path for release of fission products, which induces nucleation of stress-corrosion damage. For this reason 2D and 3D meshes are more refined in this region.

Meshes and boundary conditions

The 2D mesh is composed of 3 and 4-nodes linear elements (see Fig. 1). The box represents the refined part during the ramp, which shows the opening of the fuel crack and the closure of the gap. The radial crack in the pellet is meshed which allows to introduce contact condition between two fragments. Moreover, contact with friction is taken into account on the cladding inner surface. Finally, the pressure of the coolant (155 bar) is imposed on the external surface.

The 2D calculations are divided into two steps. At a first time, two cycles (15000 hours of irradiation) at 20 kWm⁻¹ are simulated with the 1.5D code CYRANO3 to compute the initial creep deformation under irradiation due to base operating conditions. These results are integrated in the initial geometry of the 2D mesh.

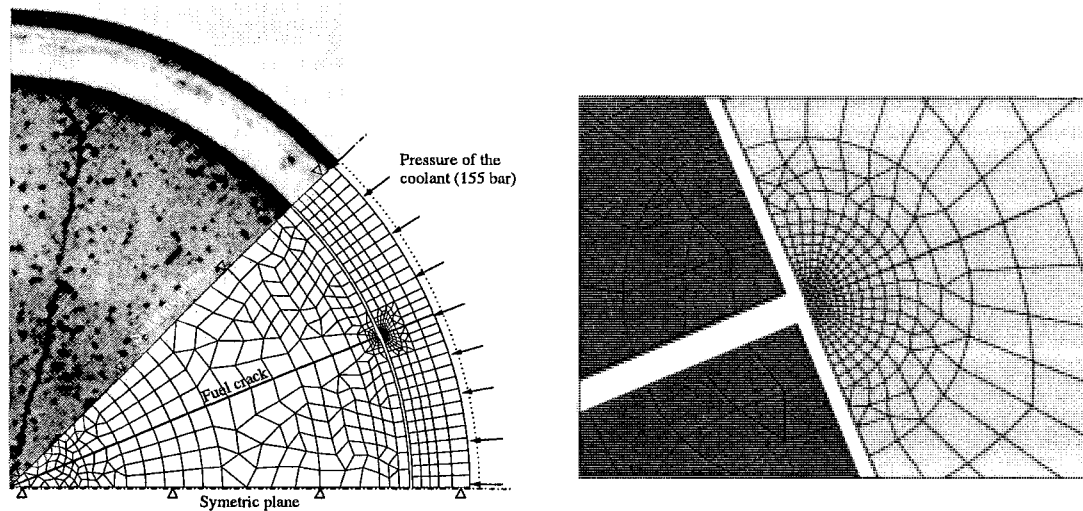


Figure 1: 2D Mesh

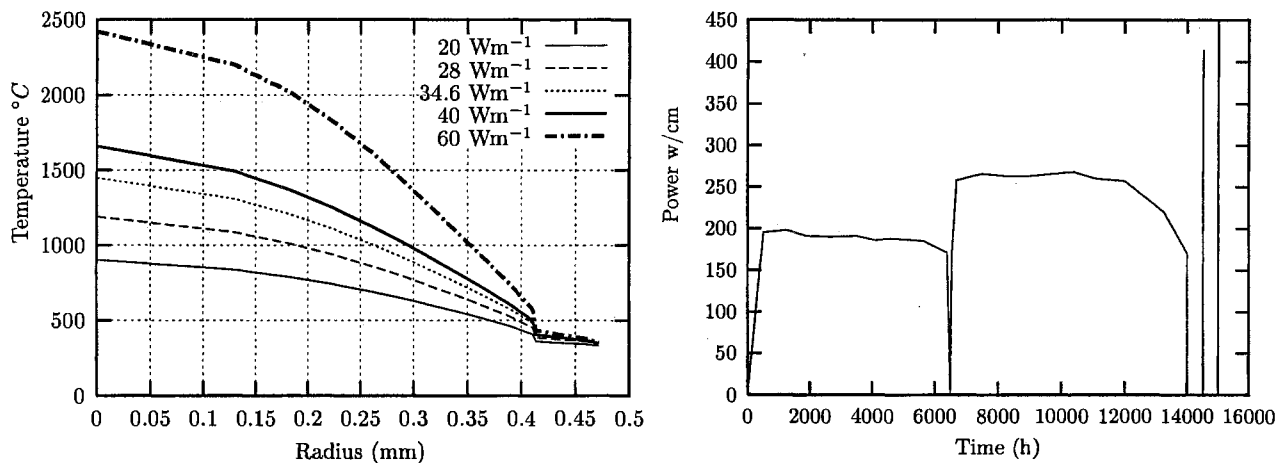


Figure 2: Calculated temperatures and power history of the 3D computation

At a second time a typical power ramp is simulated with the 2D and 3D F.E. code ZeBuLon. The imposed power history corresponds to a slow power increase up to 20 kWm^{-1} , followed by a ramp, defined by $\dot{P} = 0.17 \text{ kWm}^{-1}\text{s}^{-1}$ and $P_{max} = 40 \text{ kWm}^{-1}$ during 60 min.. In this case the effect of irradiation on the cladding mechanical behavior is not taken into account.

The 3D mesh is composed of a quarter of one fragment (due to horizontal and vertical symmetries of the fragment) and the upper part is modified to represent the pellet ridge (see Fig. 4). The structure is meshed with hexahedral and octahedral linear elements (6 and 8-nodes elements: 8500 elements and 10400 nodes). A particular attention was paid to use a regular mesh in the refined part. For this reason a specific 3D refinement method was developed with respect to more classical methods with tetrahedral elements for free meshes. Contact conditions between two fragments and between the pellet and the cladding are introduced with friction coefficients respectively of 0. and 0.8.

The 3D simulations are completely computed with the 3D F.E. code in order to obtain a 3D description of the creep deformation during the two first cycles. The two potentials corresponding to irradiation and thermal creep are used and a contact condition is chosen as criterion for the activation and deactivation of thermal and irradiation creep respectively. This method allows to unify the two models with respect to their domain of validity. For these calculations, the effect of irradiation is introduced through a dependency of the material parameters with respect to the cumulated flux.

In order to be as realistic as possible, the imposed power history is provided by irradiation measurements on a fuel rod irradiated in the Gravelines V power plant (EDF France) and ramped in the OSIRIS experimental reactor (CEA France). The power history (see Fig. 2) is composed of two cycles at 18 kWm^{-1} and 26 kWm^{-1} followed by a two ramps at 41 kWm^{-1} and 45 kWm^{-1} .

RESULTS OF THE NUMERICAL CALCULATIONS

Local response - 2D calculations

The opening of the fuel crack and the indentation of the cladding by the fuel fragments induce a maximum stress at the inner surface at the vicinity of the pellet crack. The analysis of the stress state confirms that the first eigenstress is the hoop stress. The maximum is reached at the end of the power increase. The stress decrease is due to viscoplastic deformation and relaxation. The stress evolution shows that the main part of the relaxation is achieved in the first minutes after holding the maximum power. This result is in good agreement with reported experimental times to failure. Indeed, in experimental reactors, failure occurs during the first minutes after the ramp or does not occur. This decrease of the risk of failure is due to a fast relaxation. Fractographies of unfailed rods show that this does not mean that no crack nucleates but that stress fast decreases at the tip of the crack. Profiles of stress through the cladding (Fig. 3) exhibit a high gradient in the indentation zone. Fig. 3 shows also that the maximum stress value is very sensitive to the friction conditions.

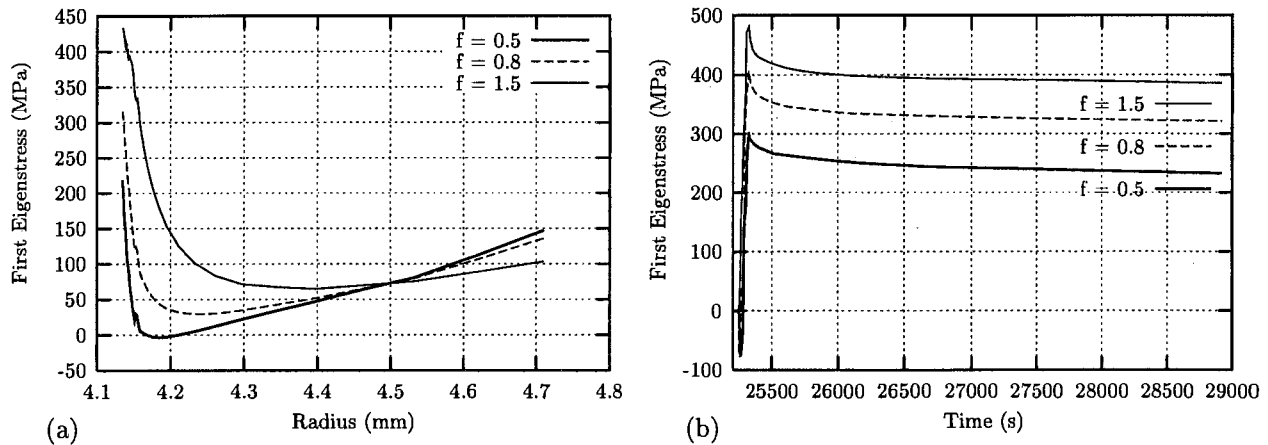


Figure 3: (a) Profile of the first eigenstress through the cladding, (b) stress relaxation in the indentation zone

Global deformation of the structure - 3D calculations

3D computations have been performed in order to take into account the 3-dimensional aspects of the pellet-cladding interaction. In this case, results are first analysed in terms of global deformation. Several computations have been performed in order to analyse the effect of the solid swelling due to fission products and the effect of a dependency of the fuel pellet thermal dilatation coefficient with the temperature. The effects of solid swelling have been introduced with an additional dilatation corresponding to about $\Delta V/V = 1.2\%$. In case of inhomogeneous dilatation coefficient, the dilatation coefficient is equal to $8.610^{-6}K^{-1}$ between 20. °C and 600. °C and reaches $12.10^{-6}K^{-1}$ at 1800. °C. Results reported in Fig. 4 show that the evolution of the fuel pellet radius is very sensitive to the dilatation coefficient distribution. In case of inhomogeneous thermal dilatation coefficient, the center of the pellet which is very hot induces an offset of the radial dilatation. This does not amplify the diabolo shape of the fuel pellet, which is the most critical parameter for the contact condition between the pellet and the cladding, but this increases the mean value of the hoop stress in the cladding. The solid swelling has only a small effect.

Filling of the fuel pellet ridge is reported in the litterature for middle and high burn-up. This phenomenon has been also studied in order to understand the contribution of creep deformation, solid and gas swelling. According to the results of Fig. 5 no filling appears after the first cycle, even with the introduction of the solid swelling. This phenomenon appears for higher burn-up and probably during long stage at high nuclear power.

The analysis of the radial profilometry of the cladding at the end of the second cycle (see Fig. 6) confirms the appearance of primary ridges and provides an estimation of their height ($\Delta\Phi = 1.8 \mu m$) with a good agreement with the experimental datas.

CONCLUSION

2D and 3D numerical simulations of the pellet-cladding mechanical interaction have been performed. The

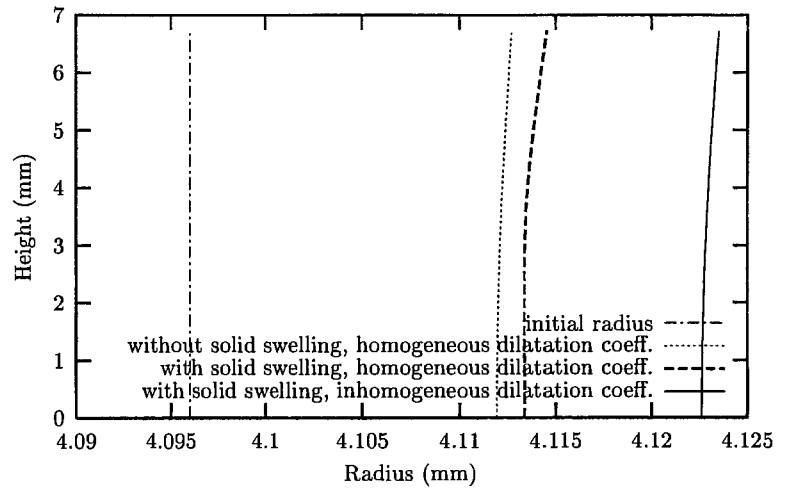
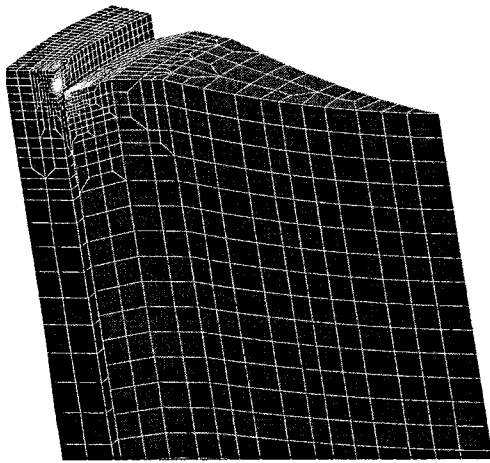


Figure 4: 3D Mesh and Fuel pellet radius at the end of the first cycle

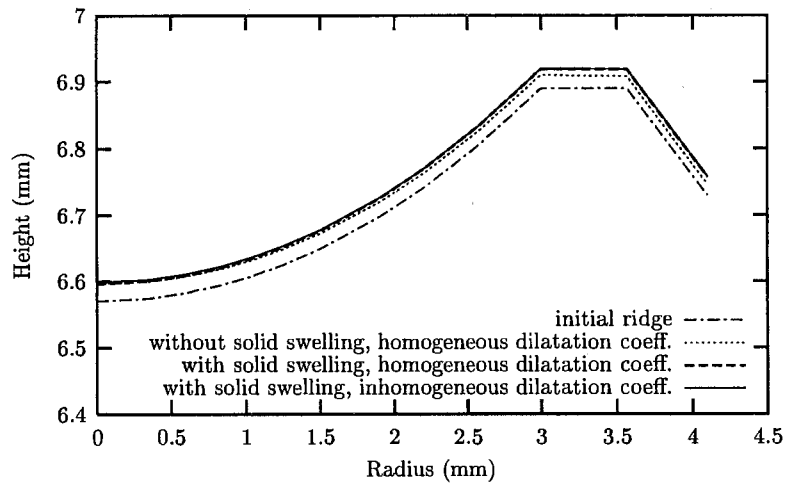


Figure 5: Fuel pellet ridge at the end of the first cycle

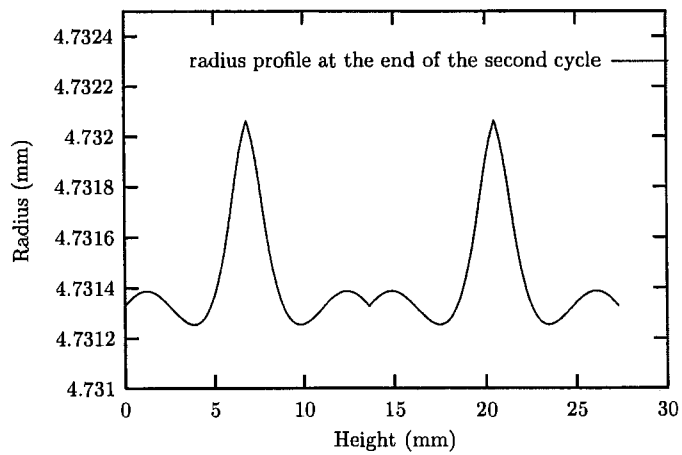
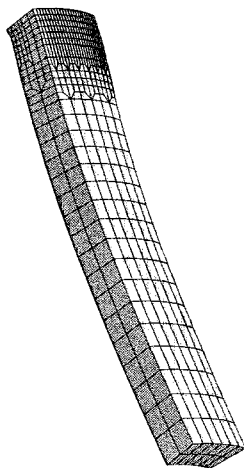


Figure 6: Primary ridge

2D computations provide good estimations of the strain and stress fields in the cladding and especially in the indentation zone. The stress concentration in this region induces a large stress gradient through the cladding which can only be described with the introduction of realistic contact and friction conditions. The sensitivity of the maximum hoop stress with the friction coefficient justifies the definition of realistic minimum and maximum friction coefficients, according to experimental observations. Moreover, the 3D computations show that the diabolo shape of the fuel pellet amplifies the indentation effect. For this reason, it is quite difficult to compute the stress and strain fields in this region. At a first time, this paper does not present those results but some geometrical aspects of the interaction. The estimation of the height of the primary ridges is in good agreement with the experimental datas and attention will be paid in the future to analyse the appearance of the secondary ridges during power ramps.

ACKNOWLEDGEMENTS

The authors would like to thank the French Atomic Energy Commission (CEA) for providing the experimental data used in this study.

References

- [1] Cubicciotti D., Jones R. L., and Syrett B. C.. Chemical aspects of iodine-induced stress corrosion cracking of zirconium. In *Zirconium in the Nuclear Industry*, ASTM STP 754, 1982, pp. 146–157.
- [2] Lynch S. P.. Environmentally assisted cracking: overview of the evidence for an adsorption-induced localised-slip model. *ActaMet*, Vol. 36 no 10, 1988, pp. 2639–2661.
- [3] Cox B.. Environmentally induced cracking of Zirconium alloys - A review. *J. Nucl. Mater.*, Vol. 170, 1990, pp. 1–23.
- [4] Wood J. C.. Factors affecting stress corrosion cracking of zircaloy in iodine vapour. *J. Nucl. Mater.*, Vol. 45, 1972, pp. 105–122.
- [5] Schuster I. and Lemaignan C.. Influence of texture on iodine-induced stress corrosion cracking of Zircalloy-4 cladding tubes. *J. Nucl. Mater.*, Vol. 189, 1992, pp. 157–166.
- [6] Miller A. K., Challenger K. D., and Tasooji A.. Scsig, a phenomenological model for iodine stress corrosion cracking of zircaloy. N. P. 1789 Vol. 1, 1981.
- [7] Williford R. E.. Chemically assisted crack nucleation in Zircaloy. *J. Nucl. Mater.*, Vol. 132, 1985, pp. 52–61.
- [8] Leclercq S.. Modelling of fuel mechanical behavior: from creep laws to internal variable models. *Nuclear Engineering and Design*, Vol. 185, 1998, pp. 221–228.
- [9] Gilbon D. and Simono C.. Effect of Irradiation on the microstructure of Zircaloy-4. In *Zirconium in the Nuclear Industry (Tenth Conference)*, ASTM STP 1280, 1994, pp. 521–548.
- [10] Fidleris V.. *J. Nucl. Mater.*, Vol. 159, 1988, pp. 22–42.
- [11] Schäffler I.. *Modélisation du comportement élasto-viscoplastique anisotrope des tubes de gaine du crayon combustible entre zéro et quatre cycles de fonctionnement en réacteur à eau pressurisée*. PhD thesis, Université de Franche-Comté, 1997.
- [12] Matthews J. R. and Finnis M. W.. Irradiation creep models. *J. Nucl. Mater.*, Vol. 159, 1988, pp. 257–285.
- [13] Oguma M.. Cracking and relocation behavior of nuclear fuel pellets during rise to power. *Nuclear Engineering and Design*, Vol. 76, 1983, pp. 35–45.